# Texture Evolution During Cold Forming of Rectangular Hollow Section

# Texture Evolution During Cold Forming of Rectangular Hollow Section

**A Kaijalainen[1], V Javaheri[1], O Nousiainen[1], J Tulonen[2], P Steen[2] and J Kömi[1]**

[1]Materials and Mechanical Engineering, Centre for Advanced Steels Research, University of Oulu, Oulu, Finland
[2]SSAB Europe, Hämeenlinna, Finland

Corresponding author email: antti.kaijalainen@oulu.fi

**Abstract**. This work aims to study the effect of cold forming on the texture evolution during the manufacturing of rectangular hollow sections. Conventional TMCP steel and a direct-quenched steel in 420 MPa strength level are compared. The texture was characterized at the centerline (S=0) and both surfaces (S=0.8) for base material, four flat side and one corner samples of the rectangular hollow section. The results show that the flat sides of both steels have the minor intensity of ~{554}<225> and ~{112}<110> texture components and an intense texture component of ~{001}<110> in the centerline. Generally, any significant difference between four flat size samples was not found and texture intensities of the conventional TMCP steel were slightly sharper compared to direct-quenched steel. The most important change is observed with the inner corner samples, where the randomly oriented texture in the base material and flat side samples changes to the {110}<111>/<112> shear texture components.

## 1. Introduction

Formed steel sections are widely used in building construction due to their relatively high strength and stiffness properties. The cold-formed and welded hollow sections which are an efficient low cost and environmentally friendly alternative for the hot-formed sections are the most popular structural steel products [1]. Cold-formed rectangular hollow sections can be fabricated out of the circular profiles in several forming stages introducing plastic deformation. The work hardening caused by plastic deformation during forming resulted in enhancing the strength and hardness although deteriorating the elongation and toughness.

Rolling texture and shear components of the bcc steels during hot rolling are broadly researched and established [2–5]. The main rolling texture components which are typically developed when austenite is deformed under plane strain conditions below its non-recrystallization temperature can be expressed as {112}<110>, {110}<110>,{111}<112> and {554}<225>, with minor amounts of {112}<131> and {100}<011> . While, shear components can be formed when austenite is deformed by rolling below its non-recrystallization temperature by developing their most popular orientations of {112}<111>, {110}<112> and {110}<111> [4].

The previous study of authors [6] showed that the impact toughness properties of a direct-quenched steel were really better than that which produced conventionally. As the continuation of that work, the aim of this study is to compare the microstructure and texture properties of that two steels which were produced

with different production routes. The main focus is the characterization of textural evolution during cold deforming from base material to the rectangular hollow section. More detailed information about the effect of cold forming parameters on the mechanical properties and microstructural changes can be found elsewhere [6,7].

## 2. Experimental material and methods

Transformation texture properties of two cold-formed structural steels to rectangular hollow sections (RHS) are investigated. The studied hot-rolled strip steels were produced by i) a conventional thermomechanical controlled processing (TMCP) and by ii) a direct quenching (DQ) process. The chemical composition of the TMCP steel was 0.07C-1.4Mn-0.02Nb-0.016Ti and DQ sample was consisted of 0.06C-0.7Mn-0.03Nb-0.002Ti (in wt.%). Tensile properties in the hot-rolled stage were quite similar, the yield strengths were ~450 MPa, tensile strengths 530-550 MPa and total elongations were 24-27 %. The microstructure of base materials was mainly ferritic structure with a small fraction of carbon-rich areas as can be seen in figure 1.

Wall thickness of RHS materials was 8 mm and the cross-section dimension was 140 x 140 mm for the TMCP sample and 150 x 150 mm for the DQ material. After forming, the external corner radius was 20 mm, which is in the middle of EN 10219 tolerance range (16-24 mm for 8 mm thickness). As same as the hot rolled condition, after forming, tensile properties in rectangular hollow sections were quite close, the yield strengths were ~550 MPa and tensile strengths ~600 MPa. However, the Charpy V impact energies at -60 °C were significantly different such that for the TMCP it was 66 J compared to 90 J for the DQ sample. More detailed information on hot-rolled strips and rectangular hollow sections can be also found in Refs. [6,7] where microstructure, cold forming rate, and mechanical properties were investigated.

The macrotexture was characterized at the centerline (S=0) and both upper and lower surfaces (S=0.8) using Rigaku SmartLab X-ray Diffractometer (XRD) for four flat sides (FS1-4) and one corner (C) samples of the rectangular hollow section. The position of the XRD samples is illustrated in figure 2. The $R_p$ value in all iterations was (conversion from measured pool graphs to computed pool graphs) less than five, therefore the results are reliable. Moreover, for the detailed investigations microtexture and microstructural characterization were studied using FESEM-EBSD acquisition and analysis (Zeiss UltraPlus FESEM and Oxford Aztec EBSD software). The EBSD measurements were performed at an accelerating voltage of 15 kV and a step size of 0.35 μm.

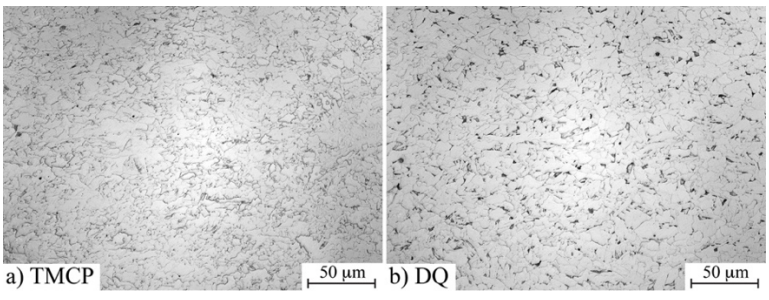


**Figure 1.** The microstructure of a) TMCP and b) DQ base material.

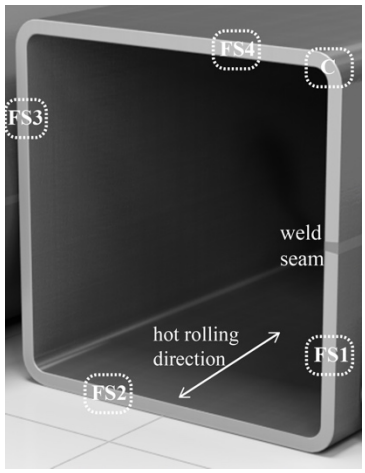


**Figure 2.** Schematic illustration of cut samples from four flat sides (FS1-4) and one corner (C) of the rectangular hollow section.

## 3. Results and discussion

### *3.1. XRD analysis*

XRD transformation textures were determined at the surfaces (S=0.8) and centerlines (S=0) for base materials and flat side and corners of rectangular hollow section specimens (figure 2), except for the centerline of TMCP base material. As no significant difference between the four flat size specimens was found, only one flat side (FS3) ODF sections are shown in figures 3 (TMCP steel) and figure 4 (DQ steel). The overall texture of both steels was weak, which is a common feature of hot rolled carbon steels. In fact, the lower surface of the both steels have almost random grain orientation. It can be seen that the texture intensities of the conventional TMCP steel were slightly sharper compared to direct-quenched steel samples. Rolling texture components (i.e. ~{554}<225>, ~{112}<110>, ~{112}<131> and ~{001}<110>) were dominant of the investigated samples, except lower/inner surface samples. The XRD results showed that the more intense ~{112}<110> and ~{001}<110> texture components were developed on the flat sides of both steels rather than the base materials. At the TMCP outer corner sample, the intensity of ~{112}<110> texture component was the most and it was the dominant texture component such that other components were almost disappeared, especially at the centerline and inner corner. Especially, in the outer surface of TMCP steel can be seen that as deformation increases the intensities of the components are increasing. The texture of the lower surface of DQ steel consists of weak texture components {112}<111> and {110}<001>. In addition, a weak non-uniform {110}<uvw> -fibre was detected in this specimen. These findings were in consistent with the earlier observed textures in the surface of hot rolled DQ steel strips [8]. It was very interesting to notice that the effect of the deformation on the texture within the centreline of the sheet and the inner surface was comparable with the deformation induced textures of the TMCP steel. All the measurements showed very weak texture at the lower/inner surface, thus more detailed EBSD microstructural characterization performed to figure out the reasons, as discussed in the next section.

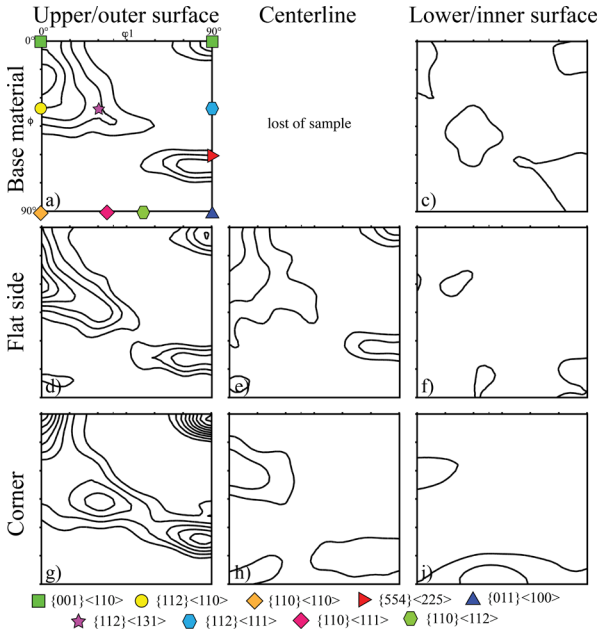


**Figure 3.** $\phi_2$=45° sections of ODFs at the upper and lower surface (S=0.8) and centerline (S=0) positions in TMCP specimens. Base material (a,c), flat side (d-f) and corner (g-i) samples. Important orientations of the bcc structure in the $\phi_2$=45° section are shown in figure a). (Levels: 1.5, 2.5,…)

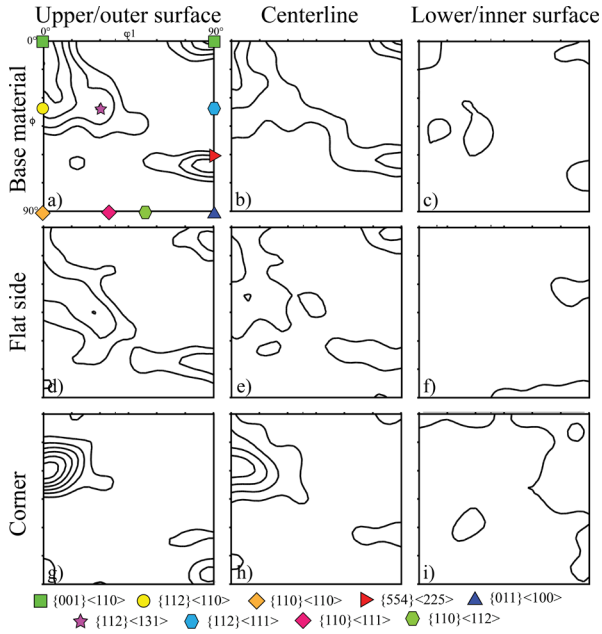


**Figure 4.** $\phi_2$=45° sections of ODFs at the upper and lower surface (S=0.8) and centerline (S=0) positions in DQ specimens. Base material (a,c), flat side (d-f) and corner (g-i) samples. Important orientations of the bcc structure in the $\phi_2$=45° section are shown in figure a). (Levels: 1.5, 2.5,…)

### *3.2. EBSD microstructure and texture analysis*

Figure 5 shows the upper/outer, centerline, and lower/inner as-rolled and corner inverse pole figures map along with the low angle and high angle grain boundaries for the TMCP steel. It can be observed that the inner grain structure is compressed, and the outer is stretched. Detailed results for the base material and RHS materials are listed in Table 1. According to the grain boundaries analysis and figure 5, the inner corner areas experienced the smallest grain sizes where the highest compression occurred. Outer corner steels showed the second smallest grain structure while centerline of corner areas had the largest grain size. The highest fraction of low-angle grain boundaries (white color in figure 5) was measured for the inner corner areas. In the case of cold forming of strip materials in Ref. [7], it has been noticed that higher straining during cold forming increases the fraction of low-angle grain boundaries, however, a similar effect cannot be seen here from the EBSD measurements, except for those inner and outer corners. Therefore, it is notable that the base material has a lot of low-angle boundaries, and conversely more deformed flat side samples have less low-angle boundaries. As can be seen from the EBSD grain size results, there are no large differences in grain sizes between investigated steels.

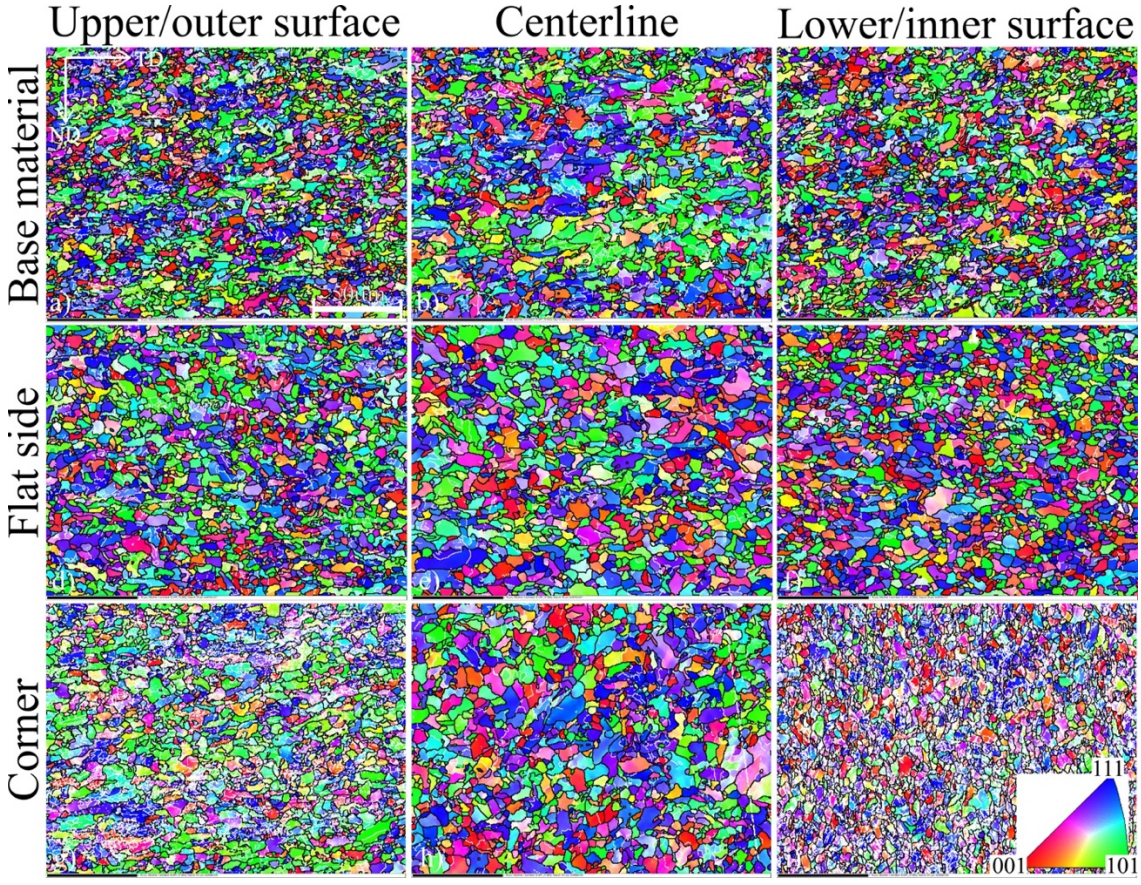


**Figure 5.** EBSD inverse pole figures (coloring in RD direction) with low- (>2.5°, white) and high-angle (15°-62.7°, black) boundaries. Microstructures of (a-c) base material, (d-f) flat side and (g-i) corner of TMCP steel. The scale bar is 50 μm. (Indexing of the patterns were between 89-95 % before clean-up)

**Table 1.** EBSD grain size of high-angle grains and fraction of low-angle boundaries.

| Material | High-angle grain size (μm) | | | Fraction of the low-angle boundaries (2.5°-15°) | | |
|---|---|---|---|---|---|---|
| | outer | center | inner | outer | center | inner |
| **TMCP base** | 3.09 | 3.91 | 3.18 | 0.28 | 0.29 | 0.24 |
| **TMCP flat side** | 3.80 | 4.49 | 3.68 | 0.24 | 0.18 | 0.12 |
| **TMCP corner** | 3.74 | 4.48 | 3.28 | 0.56 | 0.21 | 0.64 |
| **DQ base** | 4.52 | 4.83 | 4.04 | 0.14 | 0.16 | 0.36 |
| **DQ flat side** | 3.91 | 4.75 | 4.52 | 0.29 | 0.21 | 0.29 |
| **DQ corner** | 4.82 | 5.04 | 3.17 | 0.21 | 0.28 | 0.70 |

*Note: Grains below 0.78 μm are excluded from the calculation.

From the EBSD data of TMCP steel, $\phi_2$=45° sections of ODFs are calculated and results are presented in figure 6. Pole figures results are plotted in figure 7. The results were in good agreement with the XRD macrotexture indicating that the centerline of the base material has mainly the rolling texture where it increases by increasing the amount of deformation. Outer/upper surface texture intensities are weaker than centerline and also weaker than those intensities measured from the XRD data owing to the smaller investigated region. XRD is measuring a larger area than the EBSD where acquisitions are from a quite small area (200 x 150 μm). Similarly, very weak or randomly orientated texture was found for lower/inner EBSD samples compared to the XRD results.

Since the EBSD acquisitions (upper, centerline, and lower) are from the same sample, the acquisitions are obtained from the same plane which makes the job easier to determine the differences in texture between the different positions in one material. Hence, assuming only the typical bcc rolling texture at the centerline, the pole figures can clearly show the texture rotation during RHS forming. As regards, at the outer surface samples (in figures 7a, d, and g), texture shifting 10 degrees down from ~{112}<110>, which is transformed component during hot-rolling of the material. Therefore, during the cold forming process texture is sharpening and slightly increase at the centerline and outer surface of the material. However, the most significant change is observed with the inner corner samples (figure 7i), where in the base material and flat side samples the randomly oriented texture evolves to the {110}<111>/<112> and minor {112}<131> shear texture components.

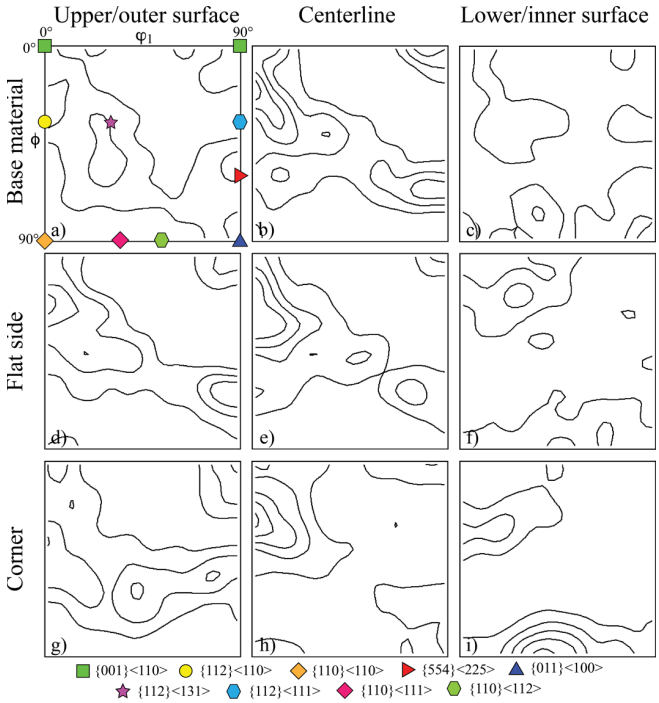


**Figure 6.** $\phi_2$=45° sections of ODFs at the upper and lower surface and centerline positions in TMCP specimens. Base material (a,c), flat side (d-f) and corner (g-i) samples. Important orientations of the bcc structure in the $\phi_2$=45° section are shown in figure a). (Levels: 1, 2,…)

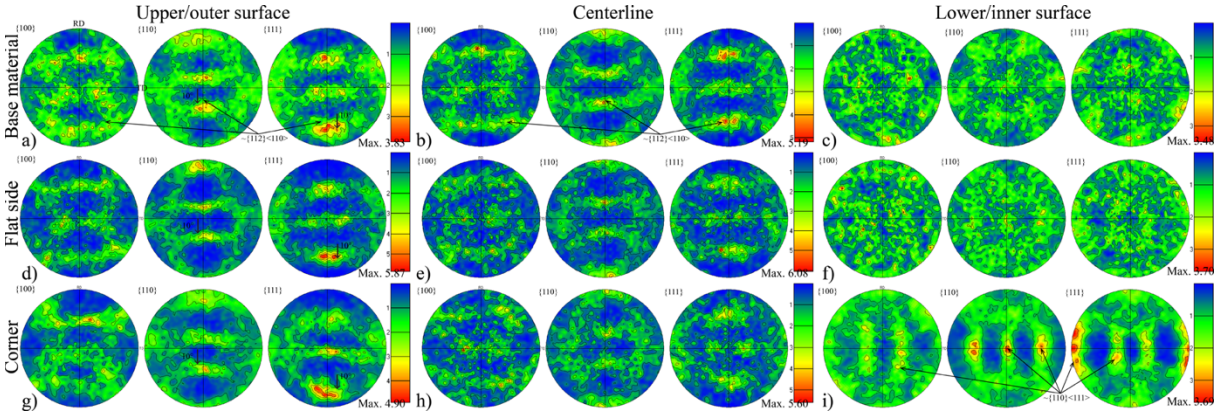


**Figure 7.** Pole figure (upper hemispheres) of the investigated material. Base material (a-c), flat side (d-f) and corner (g-i) samples.

## 4. Conclusions

The evolution of transformation texture from the base material to cold deformed rectangular hollow section during the cold forming process has been investigated. The main results can be summarized as follows:

- Inner corner areas had the smallest grain sizes with the highest compression, and the centerline areas had the largest grain size. The inner corner areas have the highest fraction of low-angle grain boundaries.
- Typically texture intensities increased as deformation increased.
- Outer surface samples texture shifted 10 degrees from ~{112}<110>, which was probably initiated during the hot rolling process.
- The most significant change was observed with the inner corner sample, such that in the base material and flat side samples the randomly oriented texture changes to the shear texture.

## References

[1] Puthli R and Packer J A 2013 Structural design using cold-formed hollow sections *Steel Constr.* **6** 150–7
[2] Ray R K and Jonas J J 1990 Transformation textures in steels *Int. Mater. Rev.* **35** 1–36
[3] Kestens L and Jonas J J 2005 Transformation and Recrystallization Textures Associated with Steel Processing *ASM Handbook vol. 14A, Metalworking: Bulk Forming* ed S L Semiatin (Materials Park: ASM International) pp 685–700
[4] Wittridge N J and Jonas J J 2000 The austenite-to-martensite transformation in Fe–30%Ni after deformation by simple shear *Acta Mater.* **48** 2737–49
[5] Kaijalainen A, Javaheri V, Lindell D and Porter D A 2018 Development of crystallographic texture under plane and shear strain in ultrahigh-strength strip steels *IOP Conf. Ser. Mater. Sci. Eng.* **375** 012026
[6] Kaijalainen A, Mourujärvi J, Tulonen J, Steen P and Kömi J 2020 Effect of direct quenching on the mechanical properties of cold formed S500 rectangular hollow section *Procedia Manuf.* **50** 777–83
[7] Kaijalainen A, Mourujärvi J, Tulonen J, Steen P and Kömi J 2021 Improvement on Impact Toughness of Cold Formed S420 Steel by Direct Quenching *Mater. Sci. Forum* **1016** 648–53
[8] Saastamoinen A, Kaijalainen A, Porter D and Suikkanen P 2017 The effect of thermomechanical treatment and tempering on the subsurface microstructure and bendability of direct-quenched low-carbon strip steel *Mater. Charact.* **134** 172–81